https://doi.org/10.31925/farmacia.2026.5.17 **ORIGINAL ARTICLE**

NETWORK PHARMACOLOGY AND *IN VITRO* ANTI-*S. EPIDERMIDIS* EFFECTS OF QUERCETIN: COMPUTATIONAL INSIGHTS INTO IL-17 SIGNALLING AND NEUTROPHIL EXTRACELLULAR TRAPS

RAMESA SHAFI BHAT *, MONA SHUJAA ALHARBI, ABEER M. AL-DBASS, SOOAD AL-DAIHAN

[1]*Biochemistry Department, Science College of King Saud University, Riyadh, Saudi Arabia*

**corresponding author: rbhat@ksu.edu.sa*

Manuscript received: July 2026

Abstract

Staphylococcus epidermidis can cause severe infections, particularly in immunocompromised patients, and its increasing antimicrobial resistance is a clinical concern. The mechanisms underlying the antibacterial activity of quercetin against this organism remain unclear. This study combined *in vitro* antibacterial assays with network pharmacology and molecular docking. Antibacterial activity was evaluated using agar well diffusion, minimum inhibitory concentration (MIC), minimum bactericidal concentration (MBC), growth-curve analysis, Fourier-transform infrared (FTIR) spectroscopy, and oxidative-stress markers in quercetin-treated *S. epidermidis*. Potential human host targets were identified using online prediction tools and evaluated by protein-protein interaction (PPI), Gene Ontology (GO), and Kyoto Encyclopaedia of Genes and Genomes (KEGG) enrichment analyses. Molecular docking was used to predict quercetin-target interactions. Quercetin exhibited concentration-dependent antibacterial activity against *S. epidermidis*, with MIC and MBC values of 125 and 500 µg/mL, respectively, sustained growth suppression, and treatment-associated FTIR changes. Network pharmacology identified 24 overlapping human host targets enriched in *IL-17* signalling and neutrophil extracellular trap formation. Molecular docking predicted favourable binding affinities between quercetin and *MMP1*, *CTSG*, *LCN2*, *CASP3*, and *ELANE*. These computational results indicate potential associations with host immune-response pathways but do not establish immunomodulatory activity. The findings demonstrate moderate direct antibacterial activity *in vitro* and provide hypothesis-generating predictions of host-response mechanisms that require experimental validation.

Rezumat

Staphylococcus epidermidis poate provoca infecții severe, în special la pacienții imunocompromiși, iar creșterea rezistenței sale la antimicrobiene reprezintă o problemă importantă. Mecanismele care stau la baza activității antibacteriene a quercetinei împotriva acestei specii nu sunt încă pe deplin elucidate. Activitatea antibacteriană a fost evaluată prin determinarea concentrației minime inhibitorii (CMI) și a concentrației minime bactericide (CMB), analiza curbelor de creștere, spectroscopie în infraroșu cu transformată Fourier (FTIR) și determinarea markerilor stresului oxidativ la *S. epidermidis* tratat cu quercetină. Potențialele ținte moleculare umane au fost identificate utilizând instrumente de predicție online și evaluate prin analiza interacțiunilor proteină-proteină (PPI), *Gene Ontology* (GO) și analiza de îmbogățire a căilor *Kyoto Encyclopedia of Genes and Genomes* (KEGG). Docking-ul molecular a fost utilizat pentru predicția interacțiunilor dintre quercetină și țintele moleculare selectate. Quercetina a prezentat o activitate antibacteriană dependentă de concentrație împotriva *S. epidermidis*, cu valori ale CMI și CMB de 125 și, respectiv, 500 µg/mL, asociată cu inhibarea susținută a creșterii bacteriene și modificări FTIR induse de tratament. Analiza prin farmacologie de rețea a identificat 24 de ținte moleculare comune ale gazdei umane, asociate predominant cu calea de semnalizare IL-17 și formarea rețelelor extracelulare ale neutrofilelor. Docking-ul molecular a evidențiat afinități de legare favorabile între quercetină și MMP1, CTSG, LCN2, CASP3 și ELANE. Aceste rezultate computaționale indică posibile asocieri cu căile implicate în răspunsul imun al gazdei, fără a demonstra însă o activitate imunomodulatoare. Rezultatele evidențiază o activitate antibacteriană directă *in vitro* moderată și generează ipoteze privind potențiale mecanisme implicate în răspunsul gazdei, care necesită validare experimentală.

Keywords: quercetin, *S. epidermidis*, network pharmacology, IL-17 signalling pathway, neutrophil extracellular trap formation

Introduction

Quercetin is a widely distributed flavonoid plant with antioxidant, antimicrobial, antiviral, and anti-inflammatory properties (1, 2). Its antimicrobial activity and the mechanisms by which it inhibits pathogenic microorganisms have been investigated extensively (3-5). Reported mechanisms include disruption of cell membranes, altered membrane permeability, inhibition of nucleic acid and protein synthesis, downregulation of virulence factors, mitochondrial dysfunction, and inhibition of biofilm formation (6, 7). Quercetin can also inhibit several drug-resistant pathogens. Its anti-inflammatory and

immunomodulatory properties support its potential pharmaceutical use, including in skin-care products (8-11). Recent studies have also examined its biological activity, therapeutic potential, and biosafety in different experimental models and biomedical applications (12-14). Quercetin can neutralise reactive oxygen species, inhibit histamine release from mast cells and basophils, and reduce the production of pro-inflammatory cytokines (15). However, its activity against bacteria that cause skin infections has received less attention. In particular, evidence concerning its activity against skin pathogens such as *S. epidermidis* remains limited, especially in the context of topical treatment.

S. epidermidis is a coagulase-negative bacterium and a common member of the skin microbiota (16). It can nevertheless cause clinically important infections, particularly in immunocompromised individuals (17). Its antimicrobial resistance and ability to form biofilms make it a major cause of medical-device-associated infections, including catheter-associated infections (18, 19). These limitations have increased interest in safe, plant-derived antimicrobial agents for topical formulations such as creams and ointments. Quercetin's biocompatibility and stability make it a potential candidate for topical formulations targeting skin infections (20), but the mechanisms by which it affects *S. epidermidis* remain incompletely understood. This study therefore investigated the effects of quercetin on *S. epidermidis*.

Network pharmacology can examine complex drug-target-pathway relationships, while molecular docking predicts interactions between compounds and proteins (21, 22). These predictions can guide subsequent experimental validation. This study combines computational and laboratory approaches to investigate the potential mechanisms of quercetin against *S. epidermidis*. To our knowledge, this is the first study combining in silico and wet-lab evidence to elucidate the multi-target mechanism of quercetin in *S. epidermidis* infection, highlighting its potential as a dual-action immunomodulatory and antibacterial agent.

Materials and Methods

Chemicals

Quercetin (purity ≥ 95%) was obtained from Sigma-Aldrich (St Louis, MO, USA).

Bacterial strain and inoculum preparation

The Gram-positive reference strain *Staphylococcus epidermidis* ATCC 12228 was used. This non-biofilm-forming strain lacks the ica operon associated with polysaccharide-mediated biofilm formation (23). The strain was cultured in freshly prepared Mueller-Hinton broth (MHB; Scharlau Chemie S.A., Barcelona, Spain) for 18 h at 37°C until the exponential growth phase. Culture turbidity was assessed by measuring the optical density at 620 nm (OD620), and the inoculum was adjusted with normal saline to a final concentration of 1.5×10^6 CFU/mL.

Antibacterial Testing

The antibacterial activity of quercetin dissolved in 70% ethanol was evaluated at 50 and 100 µg/mL using the agar well-diffusion method. Gentamicin discs (10 µg, 6-mm discs, Condalab) served as the positive control, and ethanol served as the negative control. All experiments were performed in triplicate.

Minimum inhibitory concentration (MIC)

The MIC was determined using a twofold broth-microdilution method and was defined as the lowest concentration that prevented visible bacterial growth.

Minimum bactericidal concentration (MBC)

The MBC was defined as the lowest quercetin concentration that produced no visible colony growth after subculture on agar, corresponding to 99.9% bacterial killing.

The MIC assay followed the general broth-microdilution framework described in the Clinical and Laboratory Standards Institute M07 standard, 12th edition (2024). Twofold serial dilutions of quercetin in MHB were prepared in 96-well microplates to obtain final concentrations of 1.95-1,000 µg/mL. A working *S. epidermidis* suspension of approximately 1×10^6 CFU/mL was prepared, and 100 µL was added to 100 µL of quercetin-containing medium in each well. The final volume was 200 µL, and the calculated bacterial concentration was approximately 5×10^5 CFU/mL per well, consistent with the target inoculum specified in CLSI M07. The corresponding final ethanol concentration ranged from 35% in the first well to 0.068% in the last well. The final ethanol concentrations corresponding to the MIC and MBC values were 4.37% and 17.5%, respectively. The turbidity of *S. epidermidis* growth was read after 24 hours of incubation at 37°C.

Growth curve

Staphylococcus epidermidis cultures were grown in sterile MHB containing quercetin at 50 or 100 µg/mL and incubated at 37°C with shaking at 180 rpm for 24 h. Cultures without quercetin served as controls. Optical density at 600 nm was measured hourly, and growth curves were generated by plotting optical density against time (23).

Fourier transform infrared (FTIR) spectroscopic analyses and antioxidant defence system in S. epidermidis under quercetin-induced stress

S. epidermidis cells grown in MHB containing 50 or 100 µg/mL quercetin were harvested after 24 h. The cells were centrifuged at 12,000 × g for 10 min and washed with ice-cold phosphate-buffered saline (PBS). They were then sonicated in ice-cold PBS and centrifuged at 15,000 × g for 10 min to pellet the debris. The supernatant was collected in a sterile tube for FTIR analysis and measurement of stress markers.

FTIR spectroscopy was used to examine the functional groups of cellular metabolites. Control and quercetin-exposed cells were prepared with potassium bromide and analysed using a PerkinElmer FTIR spectrometer over the range 4,000-400 cm^{-1} (24).

Reduced glutathione levels were measured using 5,5′-dithiobis (2-nitrobenzoic acid), which forms a yellow product upon reaction with sulfhydryl groups (25).

Total protein was quantified using the Bradford method, with bovine serum albumin as the standard (26).

Statistical analysis

Results are presented as the mean ± standard deviation (SD) from three independent biological replicates. Differences among groups were analysed by one-way analysis of variance in GraphPad Prism, followed by Dunnett's post hoc test where applicable. A value of $p < 0.05$ was considered statistically significant.

Network pharmacology-based analysis

Target prediction and network pharmacology of quercetin in S. epidermidis infection

Potential quercetin targets were predicted by submitting its simplified molecular-input line-entry system (SMILES) structure to SwissTargetPrediction; targets with a prediction probability ≥ 0.1 were retained. The structure-data file (SDF) for quercetin was also submitted to PharmMapper, and protein matches with a normalised fit score ≥ 0.6 were retained. To obtain infection-associated targets, GeneCards was searched using the term '*Staphylococcus epidermidis* infection', and genes with a relevance score ≥ 5 were collected. After duplicates had been removed, overlapping quercetin-predicted and infection-associated genes were identified using a Venn diagram. These genes were considered potential host targets associated with quercetin in the context of *S. epidermidis* infection.

Construction of protein-protein interaction (PPI) network

The STRING database was used to construct a protein-protein interaction (PPI) network for the predicted targets, with *Homo sapiens* selected as the organism and a minimum confidence score of 0.4. The network was visualised and analysed in Cytoscape version 3.8.1. The cytoHubba plug-in was used to identify highly connected targets and construct the regulatory network.

GO and KEGG pathway enrichment analysis

Gene Ontology (GO) and Kyoto Encyclopaedia of Genes and Genomes (KEGG) enrichment analyses were conducted in ShinyGO using the common targets. Biological process, cellular component, molecular function, and KEGG pathway categories were evaluated with a false-discovery-rate (FDR) -adjusted p-value threshold of 0.05.

Molecular docking verification

Molecular docking was performed using the AutoDock Vina-based CB-Dock server to predict interactions between quercetin and the selected host targets associated with *S. epidermidis* infection. Protein structures were selected from the Protein Data Bank on the basis of structural resolution and release date. The quercetin structure was obtained from PubChem in SDF format.

Results and Discussion

Anti-S. epidermidis activity of quercetin

The antibacterial activity of quercetin at 50 and 100 µg/mL is presented in Table I. Mean inhibition zones were 10 ± 1.0 mm and 12 ± 1.5 mm, respectively, indicating a concentration-dependent effect. The MIC and MBC were 125 and 500 µg/mL, respectively; the corresponding ethanol concentrations were 4.37% and 17.5%. In the agar-diffusion assay, the ethanol control produced a 7 ± 0.5 mm inhibition zone, whereas quercetin produced larger, concentration-dependent zones. Because matched ethanol controls were not evaluated under identical broth-microdilution conditions, the solvent may have contributed to the MIC and MBC endpoints; these values should therefore be interpreted cautiously. Quercetin also suppressed bacterial growth in liquid culture. Its inhibition zones were smaller than those produced by gentamicin (Table I). The observed moderate activity supports further investigation of quercetin as a potential adjunct or topical supportive agent rather than as a replacement for conventional antibiotics. The present *in vitro* results do not establish therapeutic or clinical efficacy.

Reported antibacterial mechanisms of quercetin include increased cell-membrane permeability, disruption of peptidoglycan assembly, and inhibition of enzymes involved in DNA replication (27-31). Quercetin can also act synergistically with β-lactam antibiotics against resistant staphylococci by inhibiting β-lactamase and enhancing drug penetration through the membrane (32-34). In the present study, growth-curve analysis showed concentration-dependent suppression of *S. epidermidis* for 24 h (Figure 1). Growth declined after 6 h at both concentrations, with greater inhibition at 100 µg/mL than at 50 µg/mL. Total protein and reduced glutathione (GSH) were measured after 24 h (Figure 2). Total crude protein decreased, particularly after exposure to 100 µg/mL quercetin, whereas GSH increased slightly.

The altered total protein and GSH concentrations indicate a cellular stress response to quercetin. The decrease in total crude protein may reflect protein damage or degradation associated with reactive oxygen species. Oxidative stress can also increase intracellular thiols and antioxidant capacity as an adaptive bacterial response (35). The slight increase in GSH

may therefore represent a thiol-based defence mechanism that helps *S. epidermidis* maintain redox balance during quercetin exposure (36-39).

Table I

Inhibition zones produced by quercetin and the controls

Strain	Inhibition zone (mm)			
	Quercetin, 50 µg/mL	Quercetin, 100 µg/mL	Ethanol (70%)	Gentamicin (10 µg)
S. epidermidis	10 ± 1.0	12 ± 1.5	7 ± 0.5	18

Values are expressed as mean ± SD (n = 3). One-way ANOVA showed a significant difference among treatment groups ($p < 0.0001$)

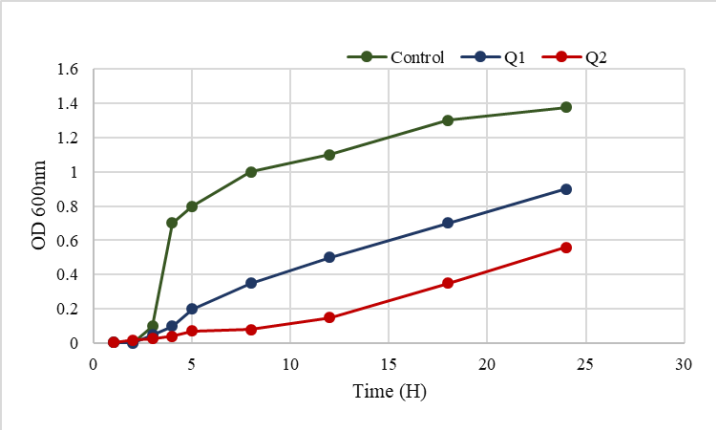


Figure 1.

Growth curves of *S. epidermidis* incubated with two different concentration of Quercetin for 24 hours

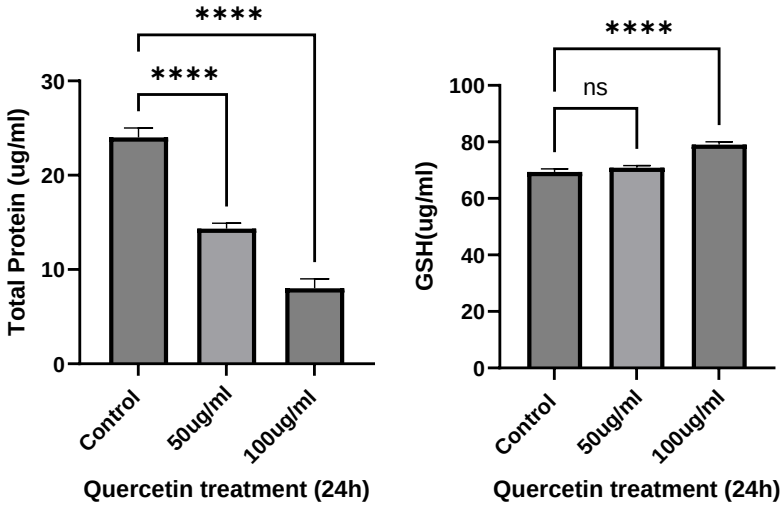


Figure 2.

Total crude protein and reduced GSH of the *S. epidermidis* strain treated with different concentration of Quercetin for 24 hours

FTIR Spectroscopy Analysis

FTIR spectroscopy was used to examine biochemical changes in quercetin-treated *S. epidermidis*. Differences in absorbance intensity and labelled bands were observed across major functional-group regions (Figure 3 and Table II). In control cells, broad bands at approximately 3,200-2,700 cm^{-1} were associated with C-H stretching in aliphatic chains and O-H stretching in fatty acids and lipids. Bands near 1,650 cm^{-1} (amide I) and 1,540 cm^{-1} (amide II) corresponded mainly to C=O stretching and N-H bending in proteins. Bands at 1,400-1,300 cm^{-1} were associated with C-H, CH_2, and CH_3 bending and carboxylic-acid C=O stretching. The 1,230-1,240 cm^{-1} region was associated with P=O stretching in phosphoryl groups and nucleic-acid phosphodiesters, whereas the 1,200-950 cm^{-1} region represented C-O-C and C-O-P stretching in cell-wall polysaccharides. Quercetin-treated cells showed differences at 3,200-2,700 cm^{-1}, suggesting possible changes in hydrogen bonding and membrane-associated lipids. Differences at 1,650-1,400 cm^{-1} may indicate changes in protein conformation, whereas changes near 1,000 cm^{-1} may reflect alterations in peptidoglycan and

surface polysaccharides. These observations indicate treatment-associated biochemical changes in quercetin-treated *S. epidermidis* cells.

For comparison, the labelled absorption bands in control cells and cells treated with 50 or 100 µg/mL quercetin are listed in Table II with their probable functional-group assignments. The principal differences occurred in the lipid (3,400-2,700 cm^{-1}), protein-associated (1,650-1,400 cm^{-1}), and polysaccharide/cell-wall (1,200-950 cm^{-1}) regions, indicating treatment-associated changes in membrane lipids, proteins, carbohydrates, and cell-wall-associated polysaccharides.

Compared with untreated cells, quercetin-treated bacteria showed differences in labelled infrared absorption bands associated with major biomolecular groups. Changes in amide-associated bands may indicate altered protein structure (40), whereas changes in lipid-associated bands are consistent with possible effects on the bacterial cell envelope (41, 42). Quercetin combined with amoxicillin has been reported to reduce fatty-acid content and alter amide signals in some Gram-positive bacteria (32). Cell-envelope alterations may increase permeability to immune factors such as lysozyme and antimicrobial peptides, and changes in protein structure may affect bacterial enzymes and other proteins (43).

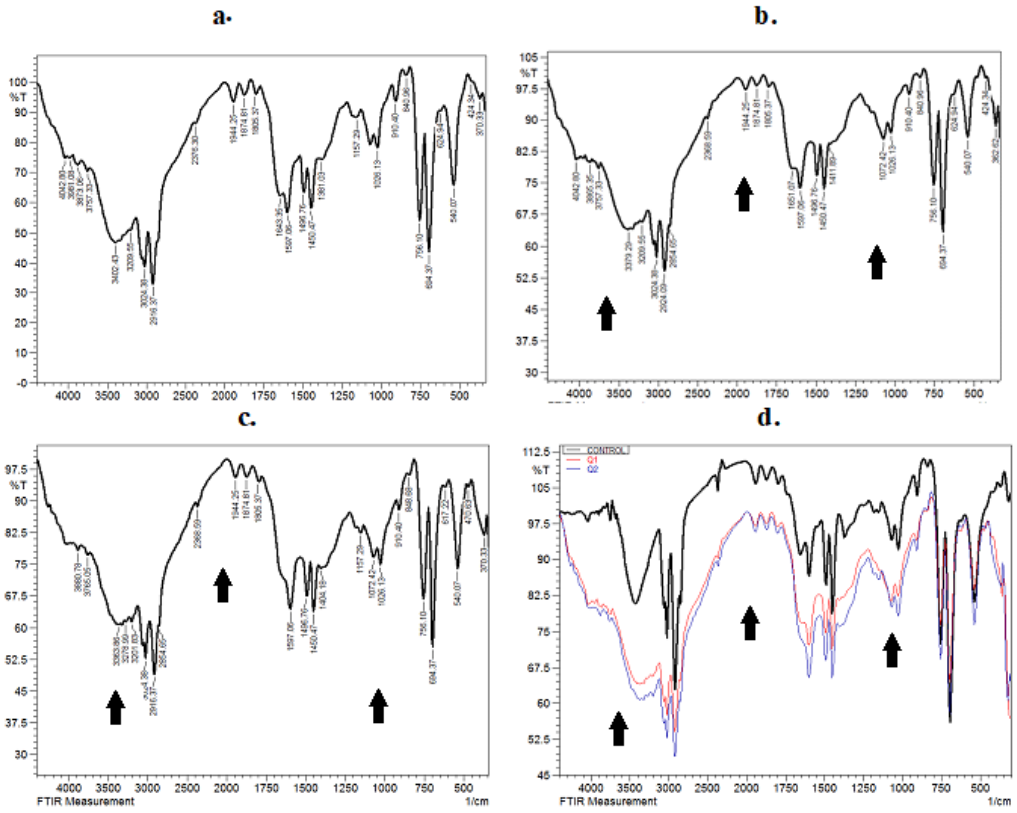


Figure 3.
FTIR spectra of *S. epidermidis* treated with quercetin for 24 h: (a) control; (b) 50 µg/mL quercetin; (c) 100 µg/mL quercetin; and (d) overlaid spectra (black, control; red, 50 µg/mL; blue, 100 µg/mL).

The experimental and computational components addressed distinct biological levels. The *in vitro* assays evaluated direct antibacterial effects on *S. epidermidis*, whereas network pharmacology and molecular docking predicted associations between quercetin and human host proteins involved in immune and inflammatory responses. The computational results therefore do not validate the mechanism underlying the antibacterial findings; they provide separate hypotheses concerning host-response pathways that require testing in appropriate human cell or *in vivo* models.

Target Prediction of Quercetin in S. epidermidis Infection

SwissTargetPrediction and PharmMapper identified 345 unique potential quercetin targets using thresholds of prediction probability ≥ 0.1 and normalised fit score ≥ 0.6, respectively. GeneCards yielded 187 genes associated with "*S.epidermidis* infection" at a relevance score ≥ 5. Comparing the Quercetin targets with *S. epidermidis* Infection genes through a Venn diagram identified 24 overlapping genes (Figure 4), which are listed with their corresponding Entrez IDs in Table III.

Table II

Labelled FTIR bands and probable functional-group assignments in control and quercetin-treated *S. epidermidis* cells

Wavenumber (cm^{-1})			**Functional group**
Control	50 µg/mL	100 µg/mL	
High-wavenumber region			
3896.83	3866.35	3880.78	Weak O-H stretching and atmospheric-water-associated region
3873.06	-	-	Weak O-H stretching and atmospheric-water-associated region
3777.33	3777.33	3765.05	Free O-H stretching vibrations
Lipids			
3402.43	3373.92	3363.86	O-H stretching (alcohols) and N-H stretching (amines and amides)
-	-	3278.99	Hydrogen-bonded O-H and N-H stretching
3209.52	3209.52	3209.52	O-H and N-H stretching
3024.38	3024.38	3024.38	=C-H stretching of unsaturated lipids
2916.37	2924.09	2916.37	C-H stretching of aliphatic CH2 and CH3 groups
-	2854.65	2854.65	Symmetric C-H stretching of CH2 groups
2376.30	2388.59	2388.59	Atmospheric CO2-associated absorption
Proteins			
1944.25	1944.25	1944.25	Overtone and combination-band region
1874.81	1874.81	1874.81	Carbonyl-related overtone and combination-band region
1806.37	1806.37	1806.37	Carbonyl-related stretching and combination-band region
1643.35	1651.07	-	Amide I band, mainly C=O stretching
1597.06	1597.06	1597.06	N-H bending and C-N stretching of protein-associated amide groups
Carbohydrates			
1496.76	1496.76	1496.76	C-H bending and aromatic C=C-associated vibrations
1450.47	1450.47	1450.47	CH2 and CH3 bending vibrations
1381.03	1411.89	1404.18	C-H bending and symmetric carboxylate stretching
1157.29	-	1157.29	C-O and C-O-C stretching of carbohydrates
Cell-wall components			
-	1072.42	1072.42	C-O, C-O-P and carbohydrate-associated stretching
1026.13	1026.13	1026.13	C-O-C and C-O stretching of polysaccharides
910.40	910.40	910.40	C-H bending of carbohydrate and cell-wall components
840.96	840.96	848.68	C-H deformation and polysaccharide-associated vibrations
756.10	756.10	756.10	C-H bending vibrations
694.37	694.37	694.37	C-H bending and fingerprint-region vibrations
624.94	624.94	617.22	C-N stretching and fingerprint-region vibrations
540.07	540.07	540.07	Fingerprint-region vibrations
424.34	424.34	470.63	Low-frequency fingerprint-region vibrations
370.33	362.62	370.33	Low-frequency fingerprint-region vibrations

All bands labelled in the individual FTIR spectra are shown. A dash indicates that no corresponding labelled band was present in that spectrum

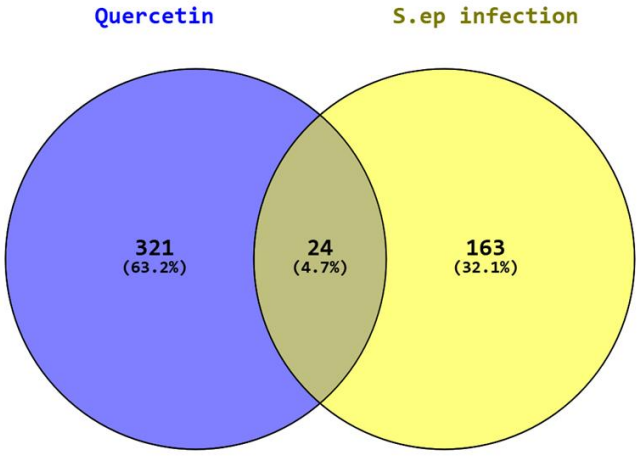


Figure 4.

Venn diagram of quercetin targets and *S. epidermidis* infection-associated genes

Table III

Potential host targets shared by quercetin and *S. epidermidis* infection-associated datasets

S.no	Symbol	Target	Entrez ID
1	*TERT*	Telomerase reverse transcriptase	O14746
2	*EGFR*	Epidermal growth factor receptor	P00533
3	*F10*	Coagulation factor X	P00742
4	*SERPINA1*	Alpha-1-antitrypsin	P01009
5	*ALB*	Albumin	P02768
6	*MMP1*	Interstitial collagenase	P03956
7	*TYMS*	Thymidylate synthase	P04818
8	*ABCB1*	ATP-dependent translocase ABCB1	P08183
9	*ELANE*	Neutrophil elastase	P08246
10	*CTSG*	Cathepsin G	P08311
11	*ALOX5*	Polyunsaturated fatty acid 5-lipoxygenase	P09917
12	*HSPA8*	Heat shock cognate 71 kDa protein	P11142
13	*ACE*	Angiotensin-converting enzyme	P12821
14	*CCL5*	C-C motif chemokine 5	P13501
15	*TYR*	Tyrosinase	P14679
16	*SELP*	P-selectin dependent granule-external membrane protein	P16109
17	*LGALS3*	Galectin-3	P17931
18	*BMP7*	Bone morphogenetic protein 7	P18075
19	*WARS1*	Tryptophan--tRNA ligase,	P23381
20	*APEX1*	DNA repair nuclease/redox regulator APEX1	P27695
21	*AHR*	Aryl hydrocarbon receptor	P35869
22	*STAT1*	Signal transducer and activator of transcription 1-alpha/beta	P42224
23	*CASP3*	Caspase-3	P42574
24	*LCN2*	Neutrophil gelatinase-associated lipocalin (NGAL)	P80188

PPI Network Analysis

The 24 predicted targets were ranked by degree (Figure 5a): *ALB, CASP3, EGFR, CCL5, LCN2, ACE, MMP1, LGALS3,SELP, CTSG, ELANE, SERPINA1, ABCB1, STAT1, TYMS, HSPA8, TERT, TYR, BMP7, F10, APEX1, WARS1, AHR*, and *ALOX5*. STRING analysis produced a PPI network containing 24 nodes and 86 edges (Figure 5b). The network was visualised in Cytoscape and arranged according to centrality measures (Figure 5c); a higher centrality value indicated greater network connectivity. CytoHubba identified *ALB, CASP3, EGFR, LCN2, CCL5, MMP1, ACE, LGALS3, SELP,* and *ELANE* as the 10 highest-ranked targets (Figure 5d).

The 24 overlapping targets were human proteins associated with immune and inflammatory responses to infection and formed an interconnected PPI network.

Gene Ontology (GO) enrichment analysis of the 24 identified common targets

The biological roles of the common targets were evaluated using ShinyGO (Figure 6). Enriched biological processes included smooth-muscle-cell proliferation, response to xenobiotic stimuli and lipids, leukocyte cell-cell adhesion, cell migration and motility, defence responses, and responses to oxygen-containing compounds and stress. These categories are consistent with host immune activation, inflammatory regulation, cellular movement, and adaptive stress responses. Enriched cellular components included the vesicle lumen, secretory-granule lumen, cytoplasmic-vesicle lumen, extracellular matrix, collagen-containing extracellular matrix, external encapsulating structure, cell surface, extracellular space, and extracellular vesicles. Molecular-function terms included macrolide binding, CCR5 chemokine-receptor binding, serine-type peptidase and endopeptidase activity, heparin and glycosaminoglycan binding, signalling-receptor activator activity, and protein homodimerization.

KEGG pathway enrichment analysis

KEGG analysis identified immune-inflammatory and infection-related pathways among the predicted targets (Figure 7). The enriched pathways included IL-17 signalling, neutrophil extracellular trap (NET) formation, MAPK signalling, and the renin-angiotensin system. Pathways labelled as epithelial-cell signalling in *Helicobacter pylori* infection, legionellosis, and toxoplasmosis may reflect shared host-defence mechanisms rather than disease-specific effects. Similarly, viral- and cancer-related pathways were enriched because they share apoptotic, chemokine, and MAPK-related components represented in the target set.

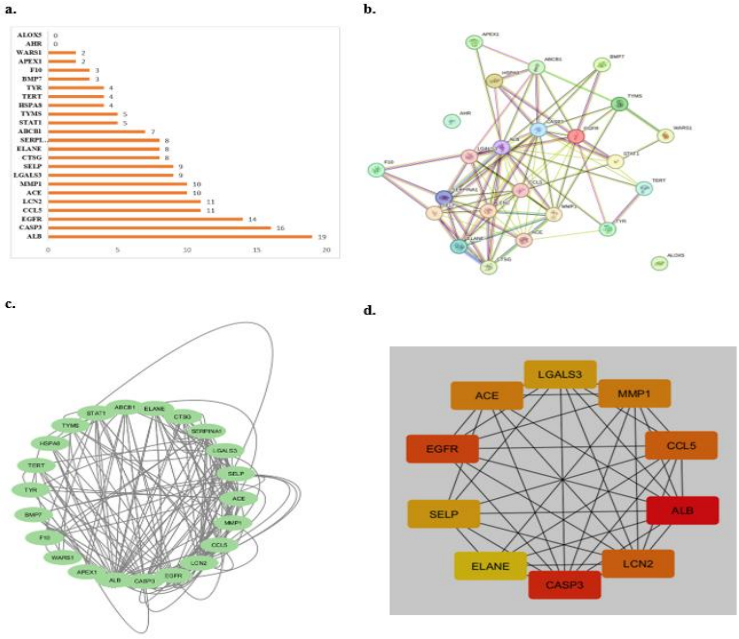


Figure 5.

PPI network analysis: (a) common targets ranked by degree; (b) STRING network of the 24 common targets; (c) network visualisation in Cytoscape; and (d) the 10 highest-ranked targets identified using cytoHubba

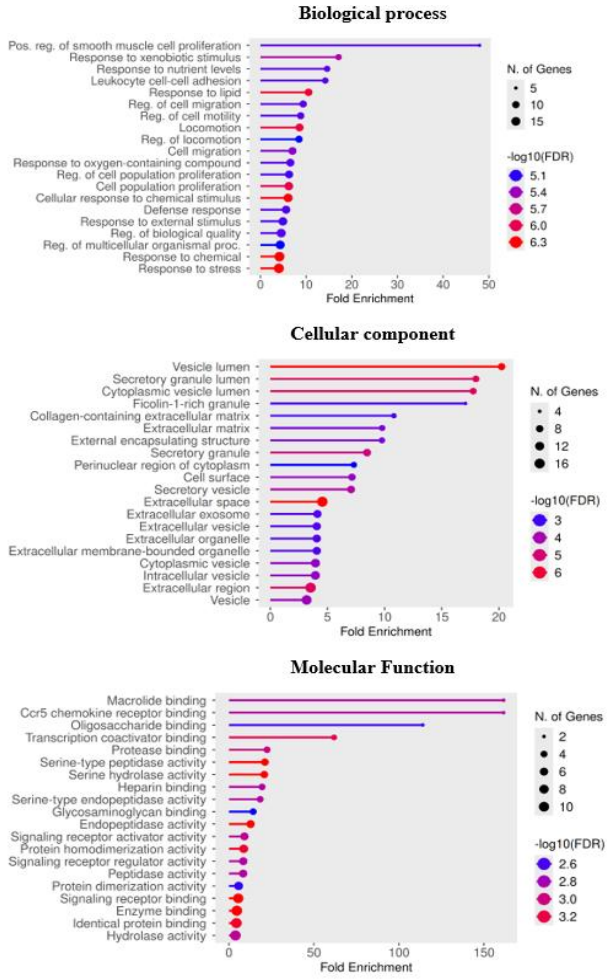


Figure 6.

GO enrichment analysis of the common targets using ShinyGO: (a) biological process; (b) cellular component; and (c) molecular function. The 20 leading terms are shown according to fold enrichment and false discovery rate

These findings suggest possible associations between quercetin and IL-17-related responses, NET formation, MAPK signalling, and epithelial defence during *S. epidermidis* infection. IL-17 signalling and NET formation were selected for pathway visualisation and molecular docking on the basis of their enrichment and hub-gene representation.

In specific, gene ontology and KEGG pathway enrichment pointed to the IL-17 signaling pathway and neutrophil extracellular trap (NET) formation as significantly enriched processes in the target network, suggesting activation of inflammation and innate immunity as main targets during staphylococcal skin infections.

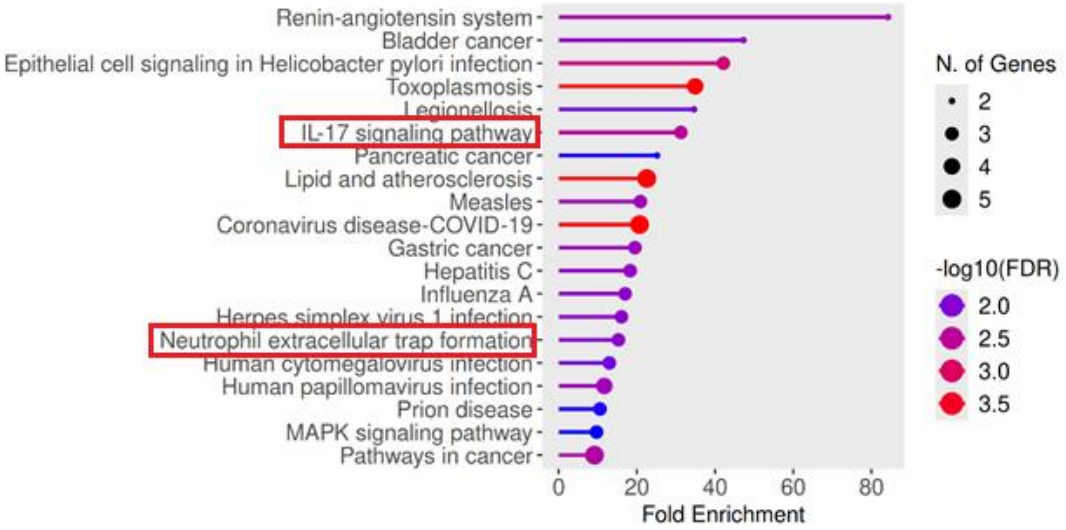


Figure 7.

KEGG pathway enrichment analysis of the common targets associated with quercetin and *S. epidermidis* infection

Identification of Core Pathways and Targets for Molecular Docking

IL-17 signalling and NET formation were the principal enriched pathways selected for further analysis. Within the IL-17 pathway, LCN2, MMP1, and CASP3 were mapped on the basis of their reported roles in antimicrobial defence, inflammatory matrix remodelling, and apoptosis (Figure 8a). ELANE and CTSG, neutrophil-derived serine proteases involved in bacterial entrapment and killing, were mapped to NET formation (Figure 8b). These five proteins were selected for docking.

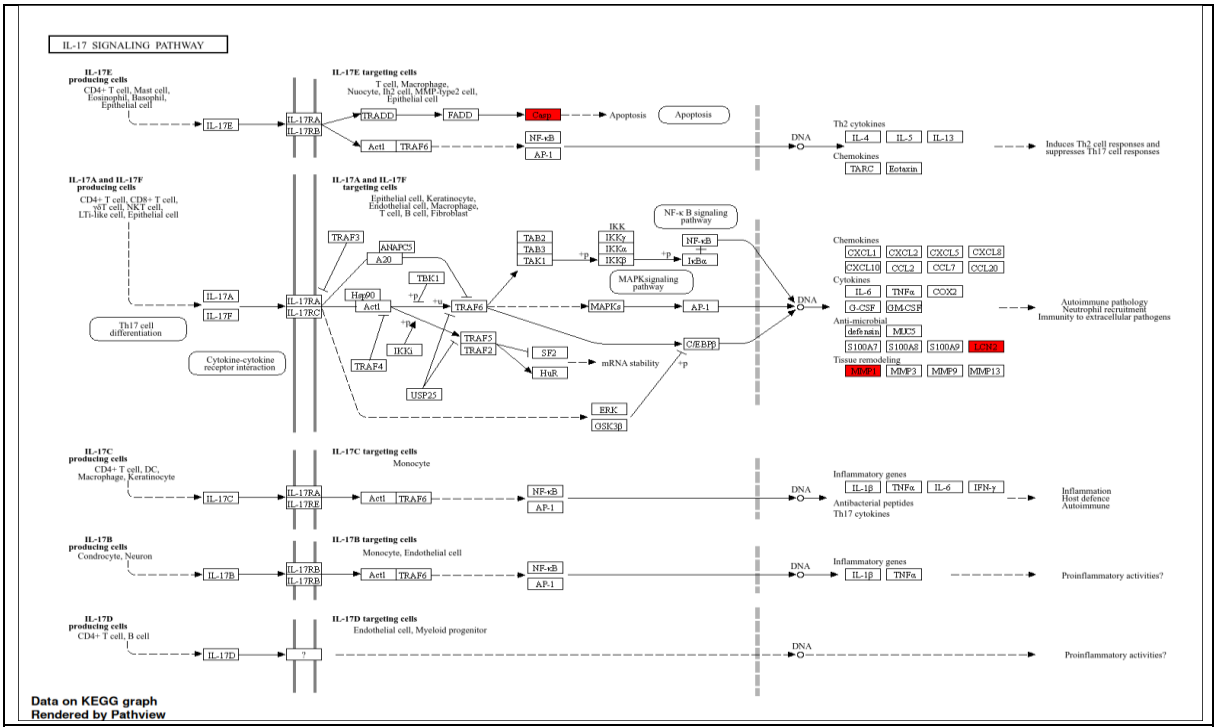
These computational associations do not demonstrate that quercetin directly regulates the selected pathways or produces a protective effect. Validation in appropriate immune-cell or *in vivo* models is required.

Lipocalin 2 (LCN2), matrix metalloproteinase 1 (MMP1), and caspase 3 (CASP3) participate in processes related to infection and inflammation (44). LCN2, also known as neutrophil gelatinase-associated lipocalin, is induced by IL-17 and IL-22 in epithelial cells and binds bacterial siderophores, thereby restricting bacterial growth (45). MMP1 is a collagenase involved in tissue remodelling and leukocyte infiltration, whereas CASP3 participates in apoptosis and may regulate the magnitude and resolution of immune responses (46). The NET pathway included neutrophil elastase (ELANE) and cathepsin G (CTSG). NETs are structures composed of DNA and granular proteins that are released by neutrophils to trap and kill microorganisms. ELANE and CTSG are incorporated into NETs and contribute to degradation of bacterial virulence factors and cell-wall components (47). In this study, the involvement of IL-17 signalling and NET formation was inferred from enrichment and docking analyses and was not experimentally confirmed. Therefore, these findings should be interpreted as predicted mechanisms. Future studies using inflammatory or immune-cell models are required to validate the regulatory effects of Quercetin on IL-17 signalling and NET-associated targets during *S. epidermidis* infection.

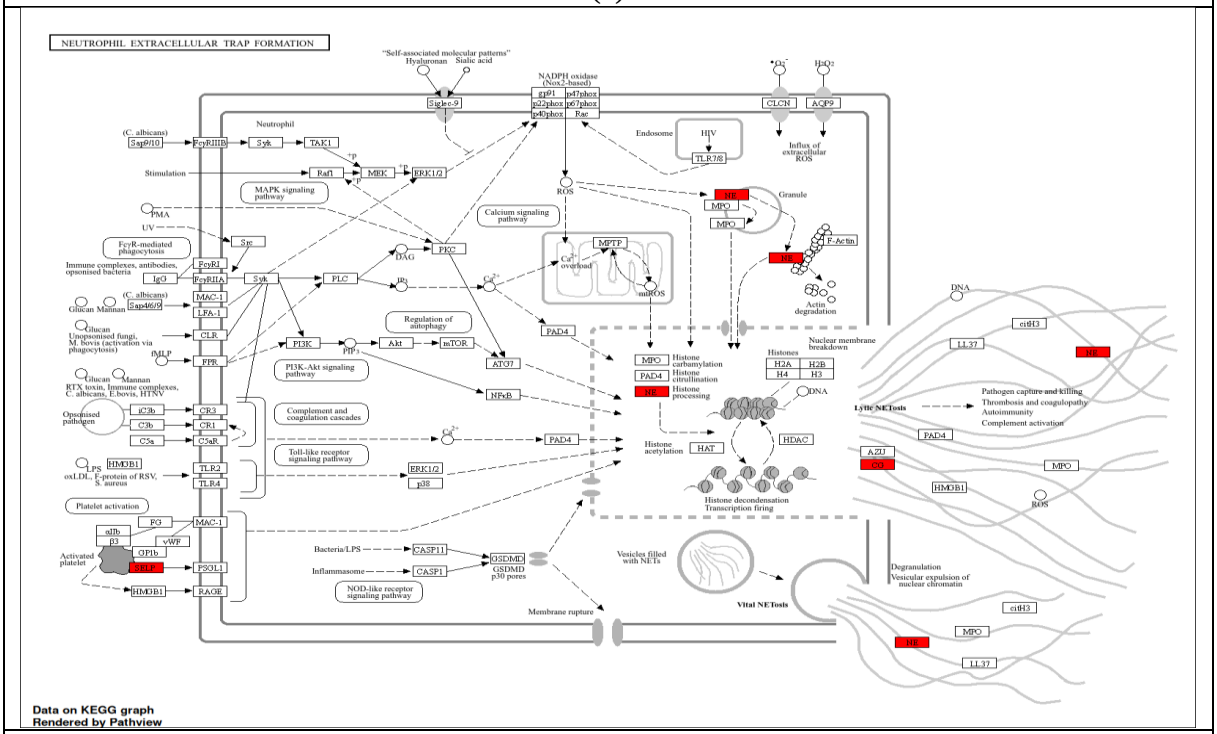
Molecular docking

Docking predicted interactions between quercetin and all selected targets (Table IV and Figure 9). For IL-17-associated proteins, predicted binding affinities were -8.5 kcal/mol for matrix metalloproteinase 1 (MMP1; PDB ID 1SU3), -7.4 kcal/mol for lipocalin 2 (LCN2; PDB ID 1DFV), and -6.0 kcal/mol for caspase 3 (CASP3; PDB ID 1PAU). For NET-associated proteins, the predicted affinities were -7.5 kcal/mol for neutrophil elastase (ELANE; PDB ID 1B0F) and -8.5 kcal/mol for cathepsin G (CTSG; PDB ID 1CGH).

MMP1 and CTSG showed the strongest predicted interactions. These *in silico* results identify candidate host targets for further investigation but do not demonstrate binding in a biological system. Quercetin has been reported to downregulate pro-inflammatory cytokines and upregulate anti-inflammatory cytokines in other experimental models (48). The relevance of those effects to *S. epidermidis* infection and to the proteins examined here requires experimental validation.



(a)



(b)

Figure 8.

Computational mapping of predicted quercetin-associated host targets in (a) the IL-17 signalling pathway and (b) the NET-formation pathway during *S. epidermidis* infection

Table IV

Predicted binding affinities of quercetin for the selected targets

Pathway	Genes	Target name	PDB ID	Affinity (kcal/mol)
IL-17 signalling	LCN2	Neutrophil gelatinase-associated lipocalin (NGAL)	1DFV	-7.4
	MMP1	Interstitial collagenase (Matrix metalloproteinase-1)	1SU3	-8.5
	CASP3	Caspase-3	1PAU	-6
NET formation	ELANE	Neutrophil elastase	1B0F	-7.5
	CTSG	Cathepsin G	1CGH	-8.5

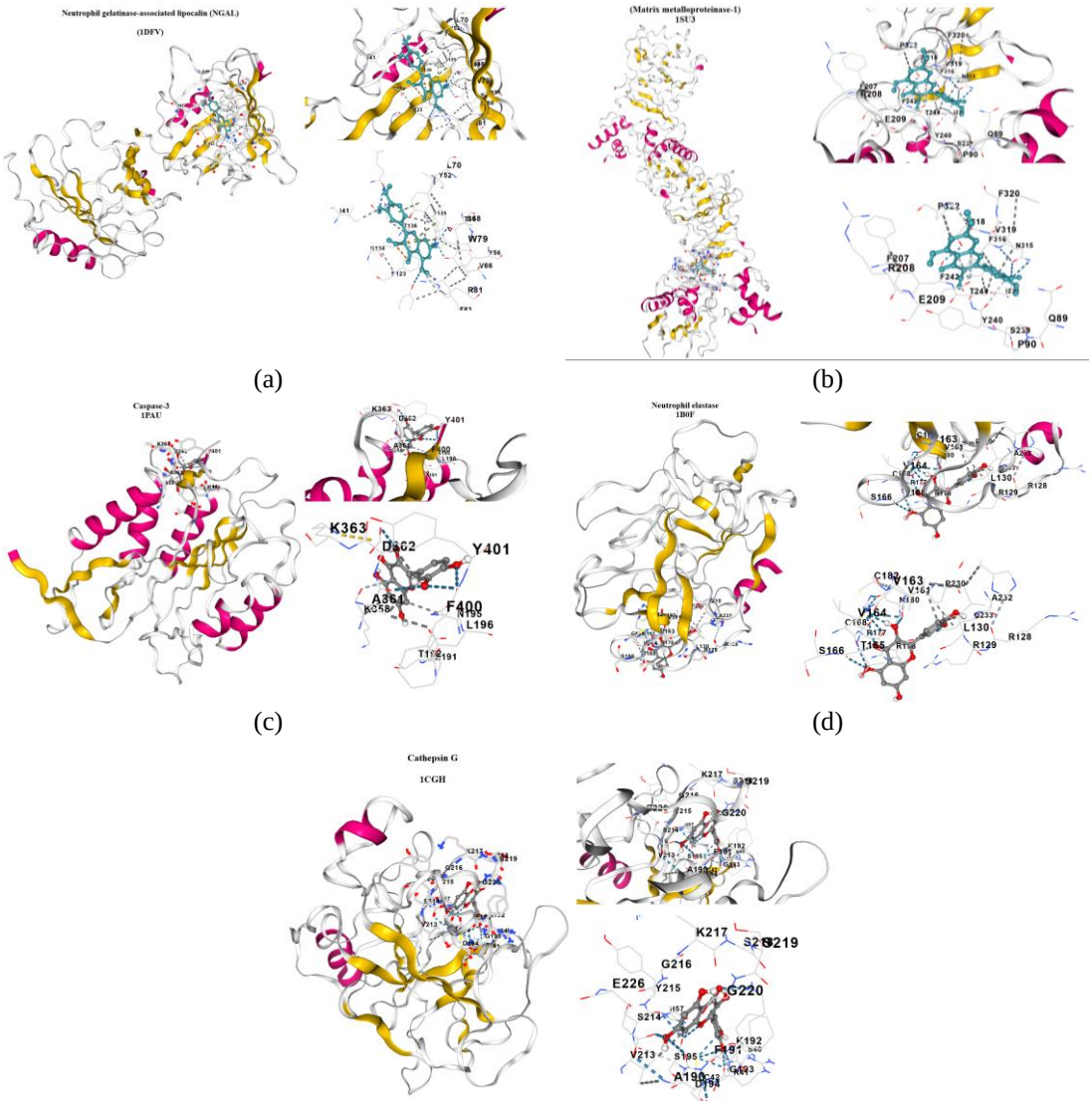


Figure 9.

Predicted docking interactions between quercetin and (a) lipocalin 2 (1DFV), (b) matrix metalloproteinase 1 (1SU3), (c) caspase 3 (1PAU), (d) neutrophil elastase (1B0F), and (e) cathepsin G (1CGH)

Conclusions

This study combined microbiological experiments within *silico* analyses to evaluate quercetin in the context of *S. epidermidis* infection. Quercetin showed moderate *in vitro* antibacterial activity, including concentration-dependent inhibition and sustained growth suppression. Computational predictions involving IL-17 signalling and NET formation suggest a possible immunomodulatory role of quercetin, which requires further experimental validation. Overall, these findings support further investigation of quercetin as a potential topical or adjunct supportive agent for inflammatory skin infections; however, its therapeutic efficacy must be established through appropriate cellular, animal, and clinical studies.

Acknowledgement

The authors extend appreciation to the Ongoing Research Funding Programme (ORF-2026-183), King Saud University, Riyadh, Saudi Arabia.

Funding

The authors extend appreciation to the Ongoing Research Funding Programme (ORF-2026-183), King Saud University, Riyadh, Saudi Arabia.

Availability of data and materials

The data generated in the present study are included in the figures and/or tables of this article.

Ethics approval and consent to participate

Not applicable.

AI use disclosure

Not applicable.

Conflict of interest

The authors declare no conflict of interest.

References

1. Alharbi HOA, Alshebremi M, Babiker AY, Rahmani AH. The role of quercetin, a flavonoid, in the management of pathogenesis through regulation of oxidative stress, inflammation, and biological activities. Biomolecules. 2025;15(1):151.
2. Aghababaei F, Hadidi M. Recent advances in potential health benefits of quercetin. Pharmaceuticals (Basel). 2023;16(7):1020.
3. Kannan S, Balakrishnan J, Govindasamy A, Arunagiri R. New insights into the antibacterial mode of action of quercetin against uropathogen Serratia marcescens in-vivo and in-vitro. Sci Rep. 2022;12(1):21912.
4. Habibi A, Pakpour Roudsari M, ZiaZiabari SM. Quercetin-conjugated magnetic nanoparticles inhibit Staphylococcus aureus growth and biofilm formation via downregulation of Coa and Hla genes. AMB Express. 2025;15(1):107.
5. Nguyen TLA, Bhattacharya D. Antimicrobial activity of quercetin: an approach to its mechanistic principle. Molecules. 2022;27(8):2494.
6. Qi W, Qi W, Xiong D, Long M. Quercetin: its antioxidant mechanism, antibacterial properties and potential application in prevention and control of toxipathy. Molecules. 2022;27(19):6545.
7. Yang D, Wang T, Long M, Li P. Quercetin: its main pharmacological activity and potential application in clinical medicine. Oxid Med Cell Longev. 2020;2020:8825387.
8. Di Petrillo A, Orru G, Fais A, Fantini MC. Quercetin and its derivatives as antiviral potentials: a comprehensive review. Phytother Res. 2022;36(1):266-278.
9. Shabir I, Kumar Pandey V, Shams R, Dar AH, Dash KK, Khan SA, et al. Promising bioactive properties of quercetin for potential food applications and health benefits: a review. Front Nutr. 2022;9:999752.
10. Okselni T, Septama AW, Juliadmi D, Dewi RT, Angelina M, Yuliani T, et al. Quercetin as a therapeutic agent for skin problems: a systematic review and meta-analysis on antioxidant effects, oxidative stress, inflammation, wound healing, hyperpigmentation, aging, and skin cancer. Naunyn Schmiedebergs Arch Pharmacol. 2025;398(5):5011-5055.
11. Manea HC, Olariu I, Predescu IA, Dumitrel SI, Kis A, Heghes A, et al. Quercetin-biosafety screening for future applications in the dental field: an in vitro and in ovo investigation. Farmacia. 2025;73(1):167-176.
12. Zaborowski MK, Dlugosz A, Blaszak B, Szulc J, Leis K. The role of quercetin as a plant-derived bioactive agent in preventive medicine and treatment in skin disorders. Molecules. 2024;29(13):3206.
13. Roman A, Boru C, Iftode A, Smeu A, Bota M, Vlaia L, et al. Genistein-quercetin combinatorial treatment yields enhanced anticancer activity in A-431 and A-375 human skin cancer cells. Farmacia. 2025;73(3):579-588.
14. Mlcek J, Jurikova T, Skrovankova S, Sochor J. Quercetin and its anti-allergic immune response. Molecules. 2016;21(5):623.
15. Sirbu MI, Predescu IA, Horhat DI, Mot IC, Banta AM, Orasan A, et al. Evaluation of quercetin, myricetin and their combination as flavonoids with antitumour potential in head and neck cancer models: an in vitro and in ovo study. Farmacia. 2025;73(5):1143-1152.
16. Severn MM, Horswill AR. Staphylococcus epidermidis and its dual lifestyle in skin health and infection. Nat Rev Microbiol. 2023;21(2):97-111.
17. Qi P, Gong F, Leng M, Wei Z. Beneficial perspective on Staphylococcus epidermidis: a crucial species for skin homeostasis and pathogen defense. Front Immunol. 2025;16:1674392.
18. Brandquist ND, Kielian T. Immune dysfunction during Staphylococcus aureus biofilm-associated implant infections: opportunities for novel therapeutic strategies. NPJ Biofilms Microbiomes. 2025;11(1):144.
19. Oliveira F, Rohde H, Vilanova M, Cerca N. Fighting Staphylococcus epidermidis biofilm-associated infections: can iron be the key to success? Front Cell Infect Microbiol. 2021;11:798563.
20. Bo Y, Li Y. Multi-target mechanisms and potential applications of quercetin in the treatment of acne vulgaris. Front Pharmacol. 2025;16:1523905.
21. Luke SS, Raj MN, Ramesh S, Bhatt NP. Network pharmacology prediction and molecular docking-based strategy to explore the potential mechanism of squalene against inflammation. In Silico Pharmacol. 2024;12(1):44.
22. Ahmad AVD, Khan SW, Ali SA, Yasar Q. Network pharmacology combined with molecular docking and experimental verification to elucidate the effect of flavan-3-ols and aromatic resin on anxiety. Sci Rep. 2024;14:9799.
23. Bhat RS, Alonazi M, Aldbass A, Al-Daihan S. The impact of varying sizes of silver nanoparticles on the induction of cellular damage in Klebsiella pneumoniae involving diverse mechanisms. Green Process Synth. 2024;13(1):20240162.

24. Bhat RS, Alghamdi JM, Aldbass AM, Aljebrin NA, Alangery AB, Soliman DA, et al. Biochemical and FT-IR profiling of Tritium aestivum L. seedlings in response to sodium fluoride treatment. Fluoride. 2022;55(1):81-89.
25. Iwasaki Y, Saito Y, Nakano Y, Mochizuki K, Sakata O, Ito R, et al. Chromatographic and mass spectrometric analysis of glutathione in biological samples. J Chromatogr B Analyt Technol Biomed Life Sci. 2009;877(28):3309-3317.
26. Bradford MM. A rapid and sensitive method for the quantitation of microgram quantities of protein utilizing the principle of protein-dye binding. Anal Biochem. 1976;72:248-254.
27. Wang S, Yao J, Zhou B, Yang J, Chaudry MT, Wang M, et al. Bacteriostatic effect of quercetin as an antibiotic alternative in vivo and its antibacterial mechanism in vitro. J Food Prot. 2018;81(1):68-78.
28. Yang X, Zhang W, Zhao Z, Li N, Mou Z, Sun D, et al. Quercetin loading CdSe/ZnS nanoparticles as efficient antibacterial and anticancer materials. J Inorg Biochem. 2017;167:36-48.
29. Pal A, Tripathi A. Quercetin potentiates meropenem activity among pathogenic carbapenem-resistant Pseudomonas aeruginosa and Acinetobacter baumannii. J Appl Microbiol. 2019;127(4):1038-1047.
30. Pal A, Tripathi A. Demonstration of bactericidal and synergistic activity of quercetin with meropenem among pathogenic carbapenem-resistant Escherichia coli and Klebsiella pneumoniae. Microb Pathog. 2020;143:104120.
31. Hossion AM, Zamami Y, Kandahary RK, Tsuchiya T, Ogawa W, Iwado A, et al. Quercetin diacylglycoside analogues showing dual inhibition of DNA gyrase and topoisomerase IV as novel antibacterial agents. J Med Chem. 2011;54(10):3686-3703.
32. Siriwong S, Teethaisong Y, Thumanu K, Dunkhunthod B, Eumkeb G. The synergy and mode of action of quercetin plus amoxicillin against amoxicillin-resistant Staphylococcus epidermidis. BMC Pharmacol Toxicol. 2016;17(1):39.
33. Luo S, Kang X, Luo X, Li C, Wang G. Study on the inhibitory effect of quercetin combined with gentamicin on the formation of Pseudomonas aeruginosa and its bioenvelope. Microb Pathog. 2023;182:106274.
34. Amin MU, Khurram M, Khattak B, Khan J. Antibiotic additive and synergistic action of rutin, morin and quercetin against methicillin-resistant Staphylococcus aureus. BMC Complement Altern Med. 2015;15:59.
35. Xu D, Hu MJ, Wang YQ, Cui YL. Antioxidant activities of quercetin and its complexes for medicinal application. Molecules. 2019;24(6):1123.
36. Kobori M, Takahashi Y, Akimoto Y, Sakurai M, Matsunaga I, Nishimuro H, et al. Chronic high intake of quercetin reduces oxidative stress and induces expression of the antioxidant enzymes in the liver and visceral adipose tissues in mice. J Funct Foods. 2015;15:551-560.
37. Granado-Serrano AB, Martin MA, Bravo L, Goya L, Ramos S. Quercetin modulates Nrf2 and glutathione-related defenses in HepG2 cells: involvement of p38. Chem Biol Interact. 2012;195(2):154-164.
38. Kinaci MK, Erkasap N, Kucuk A, Koken T, Tosun M. Effects of quercetin on apoptosis, nf-kappaB and NOS gene expression in renal ischemia/reperfusion injury. Exp Ther Med. 2012;3(2):249-254.
39. Gao WN, Pu LL, Chen M, Wei JY, Xin ZH, Wang YW, et al. Glutathione homeostasis is significantly altered by quercetin via the Keap1/Nrf2 and MAPK signaling pathways in rats. J Clin Biochem Nutr. 2018;62(1):56-62.
40. Kassem A, Abbas L, Coutinho O, Opara S, Najaf H, Kasperek D, et al. Applications of Fourier transform-infrared spectroscopy in microbial cell biology and environmental microbiology: advances, challenges, and future perspectives. Front Microbiol. 2023;14:1304081.
41. Liauw CM, Vaidya M, Slate AJ, Hickey NA, Ryder S, Martinez-Perinan E, et al. Analysis of cellular damage resulting from exposure of bacteria to graphene oxide and hybrids using Fourier transform infrared spectroscopy. Antibiotics (Basel). 2023;12(4):776.
42. Ozdil B, Guler G, Ataman E, Aktug H. Integrated spectroscopic and morphological analyses reveal cellular shifts in gene-silenced melanoma CSCs. Sci Rep. 2025;15:31175.
43. Ismail BB, He Q, Liu D, Guo M. Targeting bacterial cell envelope stress responses to advance the next generation of antimicrobial approaches. Crit Rev Food Sci Nutr. 2026;66(15):2904-2929.
44. Parmar T, Parmar VM, Perusek L, Georges A, Takahashi M, Crabb JW, et al. Lipocalin 2 plays an important role in regulating inflammation in retinal degeneration. J Immunol. 2018;200(9):3128-3141.
45. Karlsen JR, Borregaard N, Cowland JB. Induction of neutrophil gelatinase-associated lipocalin expression by co-stimulation with interleukin-17 and tumor necrosis factor-alpha is controlled by IkappaB-zeta but neither by C/EBP-beta nor C/EBP-delta. J Biol Chem. 2010;285(19):14088-14100.
46. Kazemi A, Fathy M, Jahanian A, Khanali J, Ostadi Y, Babajani A, et al. The role of MMPs and TIMPs in regenerative medicine: from pathological ECM remodeling to therapeutic applications. Biomed Pharmacother. 2025;191:118457.
47. Shahzad A, Ni Y, Yang Y, Liu W, Teng Z, Bai H, et al. Neutrophil extracellular traps (NETs) in health and disease. Mol Biomed. 2025;6(1):130.
48. Ahn HI, Jang HJ, Kwon OK, Kim JH, Oh JH, Kim SH, et al. Quercetin attenuates the production of pro-inflammatory cytokines in H292 human lung epithelial cells infected with Pseudomonas aeruginosa by modulating ExoS production. J Microbiol Biotechnol. 2023;33(4):430-440.